Doubly magic nuclei from Lattice QCD forces at M_{PS} = 469 MeV/c^2

C. McIlroy,[1,*] C. Barbieri,[1,†] T. Inoue,[2] T. Doi,[3] and T. Hatsuda[3,4]

[1]*Department of Physics, University of Surrey, Guildford GU2 7XH, UK*
[2]*Nihon University, College of Bioresource Sciences, Kanagawa 252-0880, Japan*
[3]*Theoretical Research Division, Nishina Center, RIKEN, Wako 351-0198, Japan*
[4]*iTHEMS Program and iTHES Research Group, RIKEN, Wako 351-0198, Japan*

(Dated: January 12, 2017)

We perform *ab initio* self-consistent Green's function calculations of closed shell nuclei ^{4}He, ^{16}O and ^{40}Ca, based on two-nucleon potentials derived from Lattice QCD simulations, in the flavor SU(3) limit and at the pseudo-scalar meson mass of 469 MeV/c^2. The nuclear interaction is obtained using the HAL QCD method and its short-distance nucleon-nucleon repulsion was treated by means of ladder resummations outside the model space. Comparing to previous Brueckner Hartree-Fock calculations, the total binding energies are sensibly improved by the full account of many-body correlations. The results suggest an interesting possible behaviour in which islands of stability appear at first around the traditional doubly-magic numbers when the pion mass is lowered toward its physical value. The calculated one-nucleon spectral distributions are qualitatively close to those of real nuclei even for the heavy pseudo-scalar meson mass considered here.

arXiv:1701.02607v2 [nucl-th] 11 Jan 2017

Introduction. The quantum chromodynamics (QCD) is expected to ultimately explain the structure and the interactions of all hadronic systems, together with the small corrections of electroweak origin. At the moment, systematic and non-perturbative calculations of QCD can be carried out only by Lattice QCD (LQCD). Indeed, high-precision studies have been shown to be possible e.g., in the case of single-hadron masses [1]. "Direct" calculations of multi-baryon systems have also been attempted on a lattice by several groups [2–6]. However, the typical excitation energy ΔE for multi-baryons is one to two orders of magnitude smaller than $O(\Lambda_{\rm QCD})$. Accordingly, high statistic data with very large Euclidean times $t \gtrsim \hbar/\Delta E \sim$ 10-100 fm/c is required. This is still far beyond reach due to exponentially increasing errors in t and A (the atomic number), as demonstrated theoretically and numerically in recent studies [7–9].

In this Letter, we follow a different route and perform a first *ab initio* study for medium mass atomic nuclei directly based on QCD by taking a two-step strategy. In the first step, we extract the nuclear force from *ab initio* LQCD calculations with the HAL QCD method, which generates nucleon-nucleon (NN) potentials faithful to the scattering phase shifts [10–12]. In the second step, we calculate the properties of nuclei with *ab initio* many-body methods using the LQCD potentials as input. The advantage of the HAL QCD approach is that one can extract the potential dictating all the elastic scattering states below the inelastic threshold from the lattice data for $t \gtrsim 1$ fm/c [13]. This makes the LQCD calculation of potentials affordable with reasonable statistics, together with the help of advanced computational algorithms [14–17]. We can then take the advantage of the recent developments in nuclear many-body theories to calculate various information on nuclei such as binding energies and spectral distributions. Note that a similar strategy has also been taken in Ref. [18] by applying effective field theories to LQCD data.

Recent LQCD studies in the flavor SU(3) limit by the HAL QCD collaboration have led to interactions in both the nucleon and hyperon sectors with masses of the pseudo-scalar meson (which corresponds to the pion) as low as M_{PS} =469 MeV/c^2. In these cases, potentials have been obtained for the ^{1}S$_0$ and the coupled ^{3}S$_1$-^{3}D$_1$ channels [19, 20]. Exploratory calculations based on these HAL QCD potentials were performed in the Brueckner Hartree-Fock (BHF) approach [21, 22]. This is quantitative enough to give the essential underlying physics for infinite matter but it is less reliable in finite systems. More sophisticated calculations are needed in order to go beyond the mean-field level, which is necessary to properly predict binding energies and to describe the truly complex structures of nuclei at low energy. Moreover, BHF becomes even more questionable for finite nuclei due to assumptions with the unperturbed single particle spectrum—where there is a problem in the choice between a continuous or a gap form, neither of which is completely satisfactory.

Ab initio theories for medium mass nuclei have advanced greatly in the past decade and methods such as coupled cluster and self-consistent Green's function (SCGF) are now routinely employed to study the structure of full isotopic chains up to Ca and Ni [23–26], with the inclusion of three-nucleon forces [27]. Their use with soft interactions from chiral effective field theory have led to first principle predictions of experimental total binding energies [28, 29] and nuclear radii [30–32] with unprecedented accuracies. Interactions like the HAL QCD potentials pose a bigger challenge for calculations of medium mass isotopes due to their short-distance inter-nucleon repulsion. However, the SCGF method has the advantage that two-nucleon scattering (ladder) diagrams at large momenta—needed to resolve the short-range repulsion—can be dealt with explicitly through a G-matrix [33–35].

In this Letter, we will employ the SCGF method in the third-order algebraic diagrammatic construction [ADC(3)] approximation [36–38] and use a G-matrix as the effective interaction, with some slight improvement over the formalism detailed in Ref. [35]. We find that this is accurate enough to make statements on the performance of the present HAL QCD potentials. This work is also a first step toward advancing many-body approaches that can handle hard interactions and

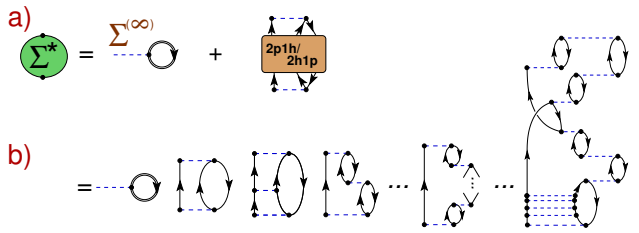

FIG. 1. (Color online) Diagrammatic content of the ADC(3) approximation. *(a)* The self-energy splits in a static mean field part and a energy dependents contribution according to Eq. (2). *(b)* The dynamic contributions are obtained as infinite resummations of ladder (pp/hh) and the ring (ph) diagrams. The ADC(3) approach includes static corrections to the coupling of nucleons to intermediate excitations (matrix **D** in Eq. (2)), an example of which is shown by the top portion of the last Goldstone diagram [38].

it will be an important direction in view of LQCD calculations that are in progress at nearly the physical pion mass [39–42].

The BHF study of Ref. [21] showed that the HAL QCD interaction in the SU(3) limit with $M_{PS} = 469$ MeV/c^2 leads to a saturated nuclear matter and it is confirmed by later SCGF calculations [43]. Thus, this is a suitable choice to investigate possible self-bound nuclei at large pion masses. In this work, we will focus on this potential and refer to it as the 'HAL469$_{SU(3)}$' interaction, or 'HAL469' for simplicity.

Formalism. We follow closely the approach of Ref. [35] and focus on the single-particle propagator given by [44, 45]:

$$g_{\alpha\beta}(\omega) = \sum_n \frac{(\mathcal{X}^n_\alpha)^* \mathcal{X}^n_\beta}{\omega - \varepsilon^+_n + i\eta} + \sum_k \frac{\mathcal{Y}^k_\alpha (\mathcal{Y}^k_\beta)^*}{\omega - \varepsilon^-_k - i\eta} \,, \qquad (1)$$

where $\mathcal{X}^n_\alpha \equiv \langle \Psi^{A+1}_n | c^\dagger_\alpha | \Psi^A_0 \rangle$ ($\mathcal{Y}^k_\alpha \equiv \langle \Psi^{A-1}_k | c_\alpha | \Psi^A_0 \rangle$) are the spectroscopic amplitudes, $\varepsilon^+_n \equiv E^{A+1}_n - E^A_0$ ($\varepsilon^-_k \equiv E^A_0 - E^{A-1}_k$) are their quasiparticle energies and $c^\dagger_\alpha (c_\alpha)$ are the second quantisation creation (annihilation) operators. In these definitions, $|\Psi^{A+1}_n\rangle$ and $|\Psi^{A-1}_k\rangle$ represent the exact eigenstates of the $(A\pm1)$-nucleon system, while E^{A+1}_n and E^{A-1}_k are the corresponding energies. We perform calculations within a spherical harmonic oscillator model space and use Greek indices, $\alpha, \beta, ...$ to label its single particle states. Within this space, the one-body propagator is obtained by solving the Dyson equation with an irreducible self-energy given by

$$\Sigma^\star_{\alpha\beta}(\omega) = \Sigma^{(\infty)}_{\alpha\beta} + \sum_{ij} \mathbf{D}^\dagger_{\alpha i} \left[\frac{1}{\omega - (\mathbf{K} + \mathbf{C}) \pm i\eta} \right]_{ij} \mathbf{D}_{j\beta} \,. \qquad (2)$$

This is the sum of a mean-field (MF) term, $\Sigma^{(\infty)}$, and the contributions from dynamical correlations. The the coupling (**D**) and interactions matrices (**K** and **C**) are computed in the ADC(3) approximation, by imposing consistency with the perturbative self-energy at third order plus infinite all-order summations of 2p1h and 2h1p configurations, as shown in Fig. 1 [36, 38]. We follow the *sc0* approximation of Refs. [35, 46], in which $\Sigma^{(\infty)}$ is calculated exactly from the fully-dressed propagator $g(\omega)$ while **D**, **K** and **C** are written in terms of a simplified MF reference propagator, $g^{REF}(\omega)$, that is chosen to best approximate $g(\omega)$ through its first two moments at the Fermi energy (see Ref. [35] for details). In practice, we solve in sequence for Eqs. (2), (1) and $g^{REF}(\omega)$, and repeat until convergence between two successive iterations.

For forces with a sizeable short-range repulsion, like the HAL QCD interactions, usual truncations of the oscillator space (of up to 12 shells in this case) are not sufficient and a resummation of ladder diagrams outside the model space is required. Our self-energy is corrected to include these contributions in two ways. First, we calculate a G-matrix according to Refs. [47, 48] and add the corresponding diagrams to its MF part, which now becomes energy dependent [35]:

$$\begin{aligned} \Sigma^{(\infty)}_{\alpha\beta}(\omega) &= \sum_{\gamma\delta} \int \frac{d\omega'}{2\pi i} G_{\alpha\gamma,\beta\delta}(\omega+\omega')\, g_{\gamma\delta}(\omega')\, e^{i\omega'\eta} \\ &= \sum_{\gamma\delta} \sum_k G_{\alpha\gamma,\beta\delta}(\omega + \varepsilon^-_k)\, \mathcal{Y}^k_\delta (\mathcal{Y}^k_\gamma)^* \,, \end{aligned} \qquad (3)$$

where $G_{\alpha\gamma,\beta\delta}(\omega)$ are the elements of the G-matrix. Secondly, we extract a static effective interaction that we use to calculate the ADC(3) self-energy (last term of Eq. (2)) within the chosen model space. To do this, we solve the Hartree-Fock (HF) equations with the MF potential of Eq. (3):

$$\sum_\beta \left\{ \langle\alpha| \frac{p^2}{2m_N} |\beta\rangle + \Sigma^{(\infty)}_{\alpha\beta}(\omega = \varepsilon^{HF}_r) \right\} \psi^r_\beta = \varepsilon^{HF}_r \psi^r_\alpha \,, \qquad (4)$$

where latin indices label HF states, and define a static interaction in this HF basis similarly to Refs. [35, 49]:

$$V_{rs,pq} = \frac{1}{2} \left[G_{rs,pq}(\varepsilon^{HF}_r + \varepsilon^{HF}_s) + G_{rs,pq}(\varepsilon^{HF}_p + \varepsilon^{HF}_q) \right] . \qquad (5)$$

The $V_{rs,pq}$ matrix elements are then transformed back to the harmonic oscillatror space to be used in the computations.

Note that the excluded space used to calculate the G-matrix is given by the full model space, so that Eq. (3) includes *only* ladder diagrams that are not already resummed in the ADC(3) computation. Thus, our G-matrix depends only on the model space and carries no ambiguity with the regards to the choice of the single-particle spectrum at the Fermi surface. Likewise, the HF results from Eq. (4) are different from the standard BHF theory, where only the occupied orbits are excluded.

It is well known that short-range repulsion, implicitly accounted by Eq. (3), has the double effect of reducing the spectral strength for dominant quasiparticle peaks and of relocating it to large momenta and large negative energies [26]. Since we cannot currently calculate for the location of strength at high momenta, it is not possible to quantify the magnitude of these two effects. However, they contribute to the Koltun sum rule for total binding energy with opposite signs and must cancel to a large extent. Thus, we chose to neglect both contributions and maintain a static $\Sigma^{(\infty)}$ to solve the Dyson equation. This is currently the major approximation in our calculations and its uncertainty is best estimated from the benchmark on ^{4}He below. Resolving it will be the subject of future work.

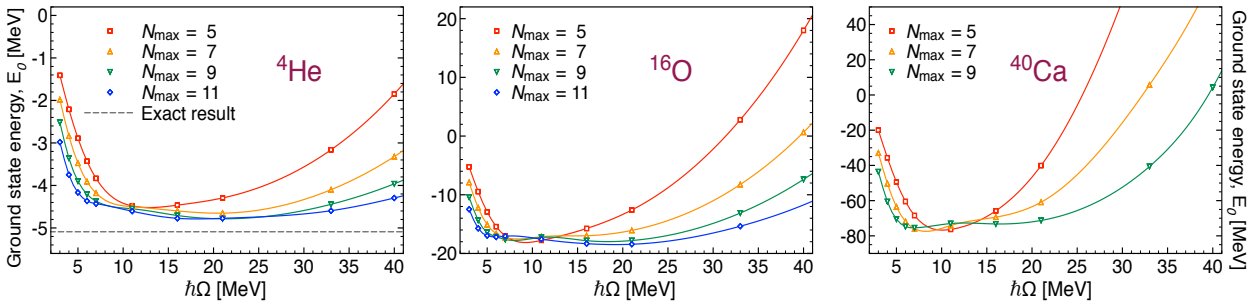

FIG. 2. (Color online) Ground state energy of ^{4}He, ^{16}O and ^{40}Ca as a function of the harmonic oscillator frequency, $\hbar\Omega$, and the model space size, $N_{\max}$. Symbols mark the results for the HAL469 potential from full self-consistent calculations in the G-matrix plus ADC(3) approach.

Results. The one-body propagators of ^{4}He, ^{16}O and ^{40}Ca were calculated in spherical harmonic oscillator spaces of different frequencies, $\hbar\Omega$, and increasing sizes up to $N_{\max}=\max\{2n+\ell\}=11$ (and $N_{\max}\leq 9$ for ^{40}Ca). A G-matrix was calculated for each frequency and model space and then it was used to derive the static interactions of Eq. (5). We subtracted the kinetic energy of the center of mass according to Ref. [50] and calculated the intrinsic ground state energy from $g(\omega)$ using the Koltun sum rule. The same lattice simulation setup used to generate the HAL469 interaction gives a nucleon mass of m_N=1161.1 MeV/c^2 in addition to the pseudo-scalar mass of M_{PS}=469 MeV/c^2. Thus, we employed this value of m_N in all the kinetic energy terms.

The exact binding energy of ^{4}He for HAL469 is known to be 5.09 MeV [51] and can be used to benchmark our approach. Fig. 2 displays the ground state energies calculated with the G-matrix plus ADC(3) method. The resummation of ladder diagrams outside the model space tames ultraviolet corrections and we find that the infrared convergence discussed in Ref. [52] applies very well for large oscillaltor frequencies. From calculations up to $\hbar\Omega$=50 MeV, we estimate a converged binding energy of 4.80(3) MeV for ^{4}He, where the error corresponds to the uncertainties in the extrapolation. All results for ^{4}He are summarised in Tab. I where we also list BHF calculations done with the same gap choice and methods of Ref. [22]. This suggests that the BHF method can overestimate the binding energy for HAL469 even sizeably. On the other hand, the full inclusion of long-range effects in ADC(3) deviates from the exact solution by less than 10%. Since the SCGF approach resums linked diagrams, and thus is size extensive, one should expect that similar errors will apply for larger isotopes. Fig. 2 also demonstrates that ^{16}O and ^{40}Ca convergence similarly to ^{4}He. Their extrapolated ground state energies are also given in Tab. I, where the first error is the uncertainties in the model space extrapolation [52]. The second error corresponds to many-body truncations and we estimate it to be 10% based on the finding for ^{4}He. The SCGF results are sensibly less bound than our previous BHF results [22]. This pattern is completely analogous to the case of ^{4}He and we interpret it as a limitation of BHF theory.

E_0^A [MeV]	^{4}He	^{16}O	^{40}Ca
BHF [22]	-8.1	-34.7	-112.7
G(ω) + ADC(3)	-4.80(0.03)	-17.9 (0.3) (1.8)	-75.4 (6.7) (7.5)
Exact Result [51]	-5.09	–	–
Separation into ^{4}He clusters:		-2.46 (0.3) (1.8)	24.5 (6.7) (7.5)

TABLE I. Ground state energies of ^{4}He, ^{16}O and ^{40}Ca at M_{PS}=469 MeV/c^2 obtained from the HAL469 interaction. 'G(ω)+ADC(3)' are the results of the present work and are compared to BHF and exact results. The last line is the breakup energy for splitting the system in ^{4}He clusters (of total energy $A/4\times$5.09 MeV).

A key feature of our calculations is the use of an harmonic oscillator space, which effectively confines all nucleons. The last line Tab. I reports the deduced breakup energies for separating the computed ground states into infinitely distant ^{4}He clusters. The ^{16}O is unstable with respect to 4-α break up, by ≈2.5 MeV. Allowing an error in our binding energies of more than 10% could make oxygen bound but only very weakly. This is in contrast to the experimental results, at the physical quarks masses, where the 4-α breakup requires 14.4 MeV. On the other hand, ^{40}Ca is stable with respect to breakup in α particles by ≈24 MeV. We expect that these observations are rather robust even when we consider the (LQCD) statistical errors in the HAL469 interaction. While such statistical fluctuations introduce additional ∼10% errors on binding energies [22], they are expected to be strongly correlated among ^{4}He, ^{16}O and ^{40}Ca. Hence, for QCD in the SU(3) limit at M_{PS}=469 MeV/c^2, we find that the deuteron is unbound [20] and ^{16}O is only just slightly above the threshold for α breakup, while ^{4}He and ^{40}Ca are instead bound. The HAL469 interaction has the lowest M_{PS} value among those considered in Refs. [19, 20], while from Ref. [21] we know that it is the only one saturating nuclear matter (although not at the physical saturation point). Moreover, we have tested that SCGF attempts at calculating asymmetric isotopes, like ^{28}O, predict strongly unbound systems even for HAL469. All these results together suggest that, when lowering of the pion mass toward its physical value, closed shell isotopes are created at first around the traditional magic numbers. This hypothesis should also be seen in the light of the limitations in the present HAL469 Hamiltonian, which was built to include

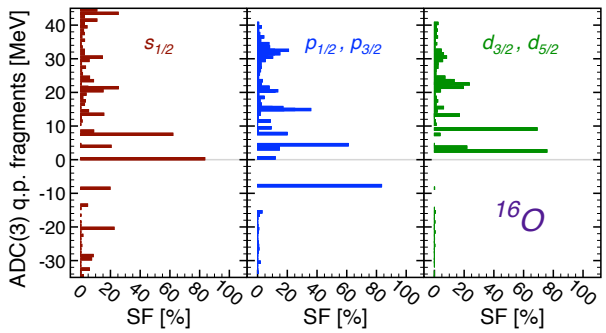

FIG. 3. (Color online) Single particle spectral strength distribution of ^{16}O obtained from the dressed propagator in the full G-matrix plus ADC(3) approach. Each panel displays partial waves of different angular momenta. The vertical axes give the quasiparticle energies (that is, the poles of Eq. (1)), while the length of the horizontal bars give the calculated spectroscopic factors.

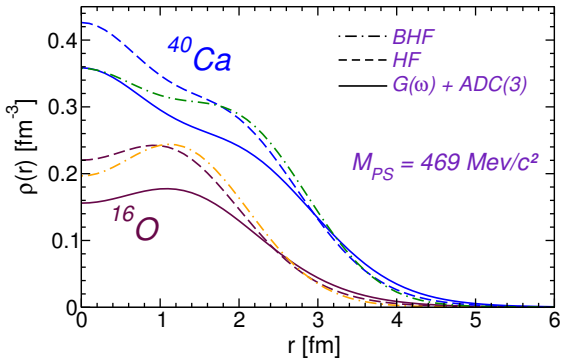

FIG. 4. (Color online) Point-matter distributions of ^{16}O and ^{40}Ca. The HF density distribution is obtained from the solutions of reference state of Eq. (4), while ADC(3) is the fully fragmented spectral function. BHF labels the results from Ref. [22].

only the $^1S_0$, $^3S_1$ and $^3D_1$ partial waves and therefore neglects the three-body forces and spin-orbit interactions.

Figure 3 demonstrates the spectral strength distributions of ^{16}O obtained for $N_{\max}$=11 and $\hbar\Omega$ = 11MeV. Quasiparticle fragments corresponding to spin-orbit partners do not split due to the absence of a spin-orbit term in HAL469. Otherwise, all the remaining qualitative features of the experimental spectral distribution are seen also for the M_{PS}=469 MeV/c^2 case. A closer look to particle-hole gaps shows that the calculated separation between the $s_{1/2}$ and $p_{1/2}$ dominant peaks in ^{16}O is 8.0 MeV, while the empirical value is 11.5 MeV. The spectral strength of ^{40}Ca is similar; however we obtain a gap of 10.1 MeV between the $f_{7/2}$ and $d_{3/2}$ states, while the experiment is 7.5 MeV. These findings are reflected in the calculated point-matter distributions and root mean square radii shown in Fig. 4 and Tab. II. Radii are larger (smaller) that the experiment for ^{16}O (^{40}Ca). The small size of calcium can be understood in terms of the higher pseudo-scalar mass that reduces the range of the Yukawa interaction. On the other hand, the large spatial extension computed for ^{16}O is consistent with the suggestion of an unbound state that would expand to infinity if the oscillator walls were removed. The HF approach of Eq. (4) and the standard BHF approaches give similar radii in spite that they predict very different binding energies (see Tab. II). However, radii are increased by full many-body correlations. For all nuclei, the full G-matrix plus ADC(3) calculations pushes the matter distribution to larger radii and reduces the central density. For charge radii in Tab. II we assumed the physical charge distributions of the proton and the neutron (see Ref. [53] for details).

Summary. We investigated the use of a G-matrix for resumming missing two-nucleon scattering diagrams outside the usual truncations of the many-body spaces, while a full *ab initio* ADC(3) approach has been retained within the model space itself. A benchmark on ^{4}He shows that the present implementation works relatively well and it allows to solve the self-consistent Green's function for the HAL QCD potentials derived from Lattice QCD. For the HAL469 force, the total binding energy agrees with the exact ^{4}He benchmark within 10% and shows that *ab initio* methods can be improved to reach large nuclei even with hard nuclear interactions.

The present accuracy is sufficient to make semi-quantitative statements on doubly magic nuclei, which are less bound compared to earlier BHF estimates. For the HAL QCD potentials we have found that the behaviour when lowering the pion mass towards the physical values is consistent with the idea that nuclei near to the traditional magic numbers are formed first. At M_{PS}=469 MeV/c^2, in the SU(3) limit of QCD, both ^{4}He and ^{40}Ca have bound ground states while the deuteron is unbound and ^{16}O decays into four separate alpha particles. However, ^{16}O is close to become bound. The calculated nuclear spectral functions reflect the different nuclear sizes (consistently with the shorter range of the Yukawa interaction) and the missing spin-orbit interactions; they are otherwise qualitatively consistent with experimental observations.

Important future work will be the inclusion the spin-orbit as well as three-nucleon forces, and LQCD calculations for these interactions are in progress [56, 57]. In addition, similar studies at physical quark masses are expected in near future, since LQCD simulations for nuclear and hyperon forces at almost physical quark masses are currently underway [39–41].

		^{16}O	^{40}Ca
$r_{pt-matter}$:	BHF [22]	2.35 fm	2.78 fm
	HF	2.39 fm	2.78 fm
	G(ω) + ADC(3)	2.64 fm	2.97 fm
r_{charge}:	G(ω) + ADC(3)	2.77 fm	3.08 fm
	Experiment [54, 55]	2.73 fm	3.48 fm

TABLE II. Computed matter and charge radii of ^{16}O and ^{40}Ca using M_{PS}=469 MeV. Results are given for different levels of approximations and the charge radii from the full G-matrix plus ADC(3) are compared to the experimental values.

Acknowledgements. We thank the HAL QCD Collaboration for providing the HAL469$_{SU(3)}$ interaction. Computations of the G-matrix were performed using the CENS codes from Ref. [48]. This work was supported in part by the United Kingdom Science and Technology Facilities Council (STFC) under Grants No. ST/L005743/1 and ST/L005816/1, by the Royal Society International Exchanges Grant No. IE150305, by Japanese Grant-in-Aid for Scientific Research (JP15K17667and (C)26400281), by MEXT Strategic Program for Innovative Research (SPIRE) Field 5, by a priority issue (Elucidation of the fundamental laws and evolution of the universe) to be tackled by using Post "K" Computer, and by the Joint Institute for Computational Fundamental Science (JICFuS). T.H. was supported partially by the RIKEN iTHEMS Program and iTHES Project. Calculations were performed at the DiRAC Data Analytic system at the University of Cambridge (BIS National E-infrastructure capital grant No. ST/K001590/1 and STFC grants No. ST/H008861/1, ST/H00887X/1, and ST/K00333X/1).

* c.s.mcilroy@surrey.ac.uk
† C.Barbieri@surrey.ac.uk

[1] S. Borsanyi, S. Durr, Z. Fodor, C. Hoelbling, S. D. Katz, S. Krieg, L. Lellouch, T. Lippert, A. Portelli, K. K. Szabo, and B. C. Toth, Science **347**, 1452 (2015).
[2] S. R. Beane, E. Chang, W. Detmold, H. W. Lin, T. C. Luu, K. Orginos, A. Parreño, M. J. Savage, A. Torok, and A. Walker-Loud (NPLQCD Collaboration), Phys. Rev. D **85**, 054511 (2012).
[3] T. Yamazaki, K.-i. Ishikawa, Y. Kuramashi, and A. Ukawa, Phys. Rev. D **86**, 074514 (2012).
[4] T. Yamazaki, K.-i. Ishikawa, Y. Kuramashi, and A. Ukawa, Phys. Rev. D **92**, 014501 (2015).
[5] K. Orginos, A. Parreño, M. J. Savage, S. R. Beane, E. Chang, and W. Detmold (NPLQCD Collaboration), Phys. Rev. D **92**, 114512 (2015).
[6] E. Berkowitz, T. Kurth, A. Nicholson, B. Joo, E. Rinaldi, M. Strother, P. M. Vranas, and A. Walker-Loud, (2015), arXiv:1508.00886 [hep-lat].
[7] T. Iritani, T. Doi, S. Aoki, S. Gongyo, T. Hatsuda, Y. Ikeda, T. Inoue, N. Ishii, K. Murano, H. Nemura, and K. Sasaki, Journal of High Energy Physics **2016**, 101 (2016).
[8] S. Aoki, T. Doi, and T. Iritani, *Proceedings, 34th International Symposium on Lattice Field Theory (Lattice 2016): Southampton, UK, July 24-30, 2016*, PoS LATTICE **2016**, 109 (2016), arXiv:1610.09763 [hep-lat].
[9] T. Iritani, *Proceedings, 34th International Symposium on Lattice Field Theory (Lattice 2016): Southampton, UK, July 24-30, 2016*, PoS LATTICE **2016**, 107 (2016), arXiv:1610.09779 [hep-lat].
[10] N. Ishii, S. Aoki, and T. Hatsuda, Phys. Rev. Lett. **99**, 022001 (2007).
[11] S. Aoki, T. Hatsuda, and N. Ishii, Progress of Theoretical Physics **123**, 89 (2010).
[12] S. Aoki, T. Doi, T. Hatsuda, Y. Ikeda, T. Inoue, N. Ishii, K. Murano, H. Nemura, and K. Sasaki (HAL QCD), PTEP **2012**, 01A105 (2012), arXiv:1206.5088 [hep-lat].
[13] N. Ishii, S. Aoki, T. Doi, T. Hatsuda, Y. Ikeda, T. Inoue, K. Murano, H. Nemura, and K. Sasaki, Physics Letters B **712**, 437 (2012).
[14] T. Doi and M. G. Endres, Computer Physics Communications **184**, 117 (2013).
[15] W. Detmold and K. Orginos, Phys. Rev. D **87**, 114512 (2013).
[16] J. Günther, B. C. Tóth, and L. Varnhorst, Phys. Rev. D **87**, 094513 (2013).
[17] H. Nemura, Computer Physics Communications **207**, 91 (2016).
[18] N. Barnea, L. Contessi, D. Gazit, F. Pederiva, and U. van Kolck, Phys. Rev. Lett. **114**, 052501 (2015).
[19] T. Inoue, N. Ishii, S. Aoki, T. Doi, T. Hatsuda, Y. Ikeda, K. Murano, H. Nemura, and K. Sasaki (HAL QCD Collaboration), Phys. Rev. Lett. **106**, 162002 (2011).
[20] T. Inoue, S. Aoki, T. Doi, T. Hatsuda, Y. Ikeda, N. Ishii, K. Murano, H. Nemura, and K. Sasaki, Nuclear Physics A **881**, 28 (2012).
[21] T. Inoue, S. Aoki, T. Doi, T. Hatsuda, Y. Ikeda, N. Ishii, K. Murano, H. Nemura, and K. Sasaki (HAL QCD Collaboration), Phys. Rev. Lett. **111**, 112503 (2013).
[22] T. Inoue, S. Aoki, B. Charron, T. Doi, T. Hatsuda, Y. Ikeda, N. Ishii, K. Murano, H. Nemura, and K. Sasaki (HAL QCD Collaboration), Phys. Rev. C **91**, 011001 (2015).
[23] V. Somà, A. Cipollone, C. Barbieri, P. Navrátil, and T. Duguet, Phys. Rev. C **89**, 061301 (2014).
[24] H. Hergert, S. K. Bogner, T. D. Morris, S. Binder, A. Calci, J. Langhammer, and R. Roth, Phys. Rev. C **90**, 041302 (2014).
[25] G. Hagen, T. Papenbrock, M. Hjorth-Jensen, and D. J. Dean, Rep. Prog. Phys. **77**, 096302 (2014).
[26] W. Dickhoff and C. Barbieri, Progress in Particle and Nuclear Physics **52**, 377 (2004).
[27] A. Carbone, A. Cipollone, C. Barbieri, A. Rios, and A. Polls, Phys. Rev. C **88**, 054326 (2013).
[28] K. Hebeler, J. Holt, J. Menéndez, and A. Schwenk, Annual Review of Nuclear and Particle Science **65**, 457 (2015).
[29] A. Cipollone, C. Barbieri, and P. Navrátil, Phys. Rev. Lett. **111**, 062501 (2013).
[30] A. Ekström, G. R. Jansen, K. A. Wendt, G. Hagen, T. Papenbrock, B. D. Carlsson, C. Forssén, M. Hjorth-Jensen, P. Navrátil, and W. Nazarewicz, Phys. Rev. C **91**, 051301 (2015).
[31] V. Lapoux, V. Somà, C. Barbieri, H. Hergert, J. D. Holt, and S. R. Stroberg, Phys. Rev. Lett. **117**, 052501 (2016).
[32] R. F. Garcia Ruiz, M. L. Bissell, K. Blaum, A. Ekstrom, N. Frommgen, G. Hagen, M. Hammen, K. Hebeler, J. D. Holt, G. R. Jansen, M. Kowalska, K. Kreim, W. Nazarewicz, R. Neugart, G. Neyens, W. Nortershauser, T. Papenbrock, J. Papuga, A. Schwenk, J. Simonis, K. A. Wendt, and D. T. Yordanov, Nat Phys **12**, 594 (2016).
[33] C. Barbieri and W. H. Dickhoff, Phys. Rev. C **65**, 064313 (2002).
[34] C. Barbieri, Phys. Lett. B **643**, 268 (2006).
[35] C. Barbieri and M. Hjorth-Jensen, Phys. Rev. C **79**, 064313 (2009).
[36] J. Schirmer, L. S. Cederbaum, and O. Walter, Phys. Rev. A **28**, 1237 (1983).
[37] C. Barbieri, D. Van Neck, and W. H. Dickhoff, Phys. Rev. A **76**, 052503 (2007).
[38] C. Barbieri and A. Carbone, "Self-consistent Green's function approaches," in *An advanced course in computational nuclear physics: Bridging the scales from quarks to neutron stars*, Lect. Notes Phys., edited by M. Hjorth-Jensen, M. P. Lombardo, and U. van Kolck (2017) Chap. 11, arXiv:1611.03923 [nucl-th].
[39] T. Doi *et al.*, *Proceedings, 33rd International Symposium on*

Lattice Field Theory (Lattice 2015): Kobe, Japan, July 14-18, 2015, PoS LATTICE **2015**, 086 (2016), arXiv:1512.01610 [hep-lat].

[40] N. Ishii *et al.*, *Proceedings, 33rd International Symposium on Lattice Field Theory (Lattice 2015): Kobe, Japan, July 14-18, 2015*, PoS LATTICE **2015**, 087 (2016).

[41] K. Sasaki *et al.*, *Proceedings, 33rd International Symposium on Lattice Field Theory (Lattice 2015): Kobe, Japan, July 14-18, 2015*, PoS LATTICE **2015**, 088 (2016).

[42] H. Nemura *et al.*, in *12th International Conference on Hypernuclear and Strange Particle Physics (HYP 2015) Sendai, Japan, September 7-12, 2015* (2016) arXiv:1604.08346 [hep-lat].

[43] A. Carbone, private communication (2015).

[44] A. Fetter and J. Walecka, *Quantum Theory of Many-particle Systems*, Dover Books on Physics (Dover Publications, 2003).

[45] W. H. Dickhoff and D. Van Neck, *Many-body theory exposed!*, 2nd ed. (World Scientific Publishing, London, 2008).

[46] V. Somà, C. Barbieri, and T. Duguet, Phys. Rev. C **89**, 024323 (2014).

[47] M. Hjorth-Jensen, T. T. Kuo, and E. Osnes, Physics Reports **261**, 125 (1995).

[48] T. Engeland, M. Hjorth-Jensen, and G. Jansen, *CENS, a Computational Environment for Nuclear Structure*, https://github.com/ManyBodyPhysics/CENS/tree/master/MBPT/ .

[49] K. Gad and H. Müther, Phys. Rev. C **66**, 044301 (2002).

[50] H. Hergert and R. Roth, Physics Letters B **682**, 27 (2009).

[51] H. Nemura, Int. Jour. Mod. Phys. E **23**, 1461006 (2014).

[52] S. N. More, A. Ekström, R. J. Furnstahl, G. Hagen, and T. Papenbrock, Phys. Rev. C **87**, 044326 (2013).

[53] A. Cipollone, C. Barbieri, and P. Navrátil, Phys. Rev. C **92**, 014306 (2015).

[54] H. D. Vries, C. D. Jager, and C. D. Vries, Atomic Data and Nuclear Data Tables **36**, 495 (1987).

[55] I. Angeli and K. Marinova, Atomic Data and Nuclear Data Tables **99**, 69 (2013).

[56] K. Murano, N. Ishii, S. Aoki, T. Doi, T. Hatsuda, Y. Ikeda, T. Inoue, H. Nemura, and K. Sasaki, Physics Letters B **735**, 19 (2014).

[57] T. Doi, S. Aoki, T. Hatsuda, Y. Ikeda, T. Inoue, N. Ishii, K. Murano, H. Nemura, K. Sasaki, and HAL QCD Collaboration, Progress of Theoretical Physics **127**, 723 (2012).